FUDMA Journal of Sciences (FJS)
ISSN online: 2616-1370
ISSN print: 2645 - 2944
Vol. 10 No. 7, March, 2026, pp 27 – 35
DOI: https://doi.org/10.33003/fjs-2026-1007-5154

INTEGRATED NMR, FTIR, AND MASS SPECTROMETRIC APPROACH TO THE STRUCTURAL ELUCIDATION OF A HEPTACYCLIC METHOXY- AND METHYLPEROXY-SUBSTITUTED COMPOUND FROM *Lactuca taraxacifolia*

***[1]Benedict C. Anyanwu, [2]Chidi P. Njoku, [1]Canice U. Silas, [3]Onyinyechi U. Akoh, [3]Bright C. Onyekwere and [1]Gogo C. Anyanwu**

[1]Department of Chemistry, Kingsley Ozumba Mbadiwe University, Ideato Imo State, Nigeria.
[2]Department of Chemistry, Alvan Ikoku Federal University of Education, Imo State, Nigeria.
[3]Department of Chemistry, Michael Okpara University of Agriculture, Abia State, Nigeria.

*Corresponding authors' email: anyanwubenedict5@gmail.com

ABSTRACT

This study reports the extraction, isolation, and spectroscopic characterization of compound SB2 from the aerial parts of *Lactuca taraxacifolia*. Pulverized plant material was extracted with chloroform and successively partitioned using n-hexane, trichloromethane, ethyl ethanoate, and methanol. The trichloromethane fraction was subjected to silica gel column chromatography using a gradient solvent system of n-hexane and ethyl ethanoate (100:0–0:100, v/v). Fractions were monitored by thin-layer chromatography using n-hexane/ethyl ethanoate (9:1, v/v) as the mobile phase, yielding SB2 as a green oily liquid with a single spot (Rf = 0.42). Structural characterization was carried out using FTIR, ^{1}H NMR, ^{13}C NMR, COSY, and GC–MS analyses. GC–MS revealed a molecular ion peak at m/z 530.7804 corresponding to the molecular formula $C_{36}H_{50}O_3$. Spectroscopic data indicated the presence of aromatic and aliphatic domains together with oxygenated functionalities including methoxy and methylperoxy groups. Although overlapping NMR signals limited definitive structural assignment, the combined GC–MS, FTIR, and NMR data support a structurally complex oxygenated aromatic–aliphatic compound with possible polycyclic features. The findings contribute to the phytochemical knowledge of Lactuca *taraxacifolia*.

INTRODUCTION

Lactuca taraxacifolia (also known as *Launaea taraxacifolia*), commonly referred to as wild lettuce, is an herbaceous plant belonging to the *Asteraceae* family. It is a perennial or semi-perennial species native to tropical Africa and widely distributed across Nigeria, Ghana, Senegal, and Sierra Leone (Adinortey *et al*., 2018). The plant thrives in open grasslands, roadsides, and well-drained soils, and is morphologically characterized by a basal rosette of lanceolate to oblong leaves with slightly serrated margins and a characteristic milky latex exudate. Its yellow ligulate flower heads produce wind-dispersed seeds, contributing to its ecological adaptability (Lebeda *et al*., 2004).

In West Africa, *L. taraxacifolia* is both a nutritional and medicinal plant. The leaves are consumed as vegetables in soups and salads and are locally known as ego yarin (Yoruba, Nigeria), namijindayi (Hausa), and agbioke (Ghana) (Adinortey *et al.*, 2018). Ethnomedicinally, the plant is used in the treatment of malaria, fever, hypertension, diabetes, infections, and inflammatory conditions. Its widespread traditional use highlights its importance in local healthcare systems and supports continued phytochemical investigation (Koukoui *et al*., 2015).

Previous phytochemical studies have reported the presence of flavonoids, saponins, alkaloids, terpenoids, tannins, steroids, and glycosides in *L. taraxacifolia*, indicating a rich reservoir of bioactive secondary metabolites (Anyanwu *et al*., 2022). In particular, Anyanwu *et al.* reported the isolation of secondary metabolites from the aerial parts of *Lactuca taraxacifolia* using similar extraction and chromatographic techniques as those employed in the present study. However, while both studies utilize comparable methodologies, the isolated compounds differ in their molecular characteristics, as evidenced by distinct chromatographic behaviour and molecular ion peaks. This indicates that *L. taraxacifolia* produces multiple chemically distinct metabolites that are yet to be fully characterized. Notably, both compounds share structural similarity in possessing methoxy substituents attached to a cyclohexane ring system. Nevertheless, a key point of divergence lies in their functional group composition: the compound reported by Anyanwu *et al*. contains a carbonyl substituent, whereas the compound obtained in the present study is characterized by the presence of a methyl peroxyl substituent. This variation further emphasises the chemical diversity of metabolites derived from *L. taraxacifolia.*

Polycyclic natural products are of considerable interest due to their diverse biological activities, including antimicrobial, anti-inflammatory, and anticancer properties (Newman & Cragg, 2020). Members of the Asteraceae family are well known for producing structurally diverse secondary metabolites, particularly sesquiterpene lactones and related oxygenated compounds, making them important targets in natural product research. Consequently, further investigation of *Lactuca taraxacifolia* may reveal additional structurally unique compounds with pharmacological relevance (Salazar-Gómez *et al.*, 2020).

The present study therefore aims to isolate and characterize a secondary metabolite from the aerial parts of *L. taraxacifolia*. The specific objectives are to extract and fractionate the crude trichloromethane extract using solvent partitioning techniques, isolate compounds using column chromatography, assess purity using TLC, and characterize the isolated compound using FTIR, ^{1}H NMR, ^{13}C NMR, COSY, and GC–MS techniques. Through this approach, the study reports the characterization of a distinct metabolite, SB2, contributing further to the phytochemical understanding of this species.

MATERIALS AND METHODS

Experimental

All solvents were of analytical grade and distilled prior to use. Silica gel (200 mesh) was used for column chromatography,

and analytical TLC was performed on silica gel plates (Merck 60 F254). FTIR spectra were recorded on an Agilent Technologies Cary 630 FTIR spectrophotometer using potassium bromide pellets. NMR spectra were acquired on a Bruker Avance 400 MHz spectrometer in deuterated chloroform ($CDCl_3$), with tetramethylsilane (TMS) as internal standard. GC–MS analysis was performed using an Agilent 7890A gas chromatograph equipped with an HP-5 MS capillary column (Grootveld *et al*., 2019; Lovestead & Urness, 2019).

Plant Material Collection, Identification, and Preparation

Fresh aerial parts of *Lactuca taraxacifolia* were collected from a farm in Ogbomosho, Oyo State, Southwestern Nigeria. The plant was authenticated by Dr. C. Ibeh of the Taxonomy Section, Department of Plant Science and Biotechnology, Michael Okpara University of Agriculture, Umudike, Nigeria. A voucher specimen (MOUAU/CHEM/PLT/2018/022) was deposited in the departmental herbarium for reference. The plant material was air-dried at ambient laboratory temperature (28 ± 2 °C) under shade to prevent photodegradation, pulverized, and stored in an airtight container prior to extraction (Harborne, 1998).

Extraction and Isolation

Precisely 1.5 Kg of air-dried and pulverized aerial parts of *Lactuca taraxacifolia* were extracted at room temperature using chloroform (3 × 3 L) over 72 h with occasional shaking. The combined extracts were filtered and concentrated under reduced pressure at 38 °C using a rotary evaporator to yield a dark-green approximately 95 g of crude extract (Azwanida, 2015). The crude extract was suspended in about 300 mL of distilled water and successively partitioned with n-hexane, trichloromethane, ethyl ethanoate, and methanol (3 × 300 mL each). Precisely 22 g of trichloromethane fraction, which exhibited multiple UV-active spots on TLC, was subjected to silica gel column chromatography (200 mesh) (Sherma, 2019; Sirin, 2017).

Elution was carried out using a gradient system of n-hexane and ethyl ethanoate (100:0 to 0:100, v/v) (Sherma, 2019). Fractions were monitored by TLC using n-hexane/ethyl ethanoate (9:1, v/v) as the mobile phase. Similar fractions were pooled based on TLC profiles and concentrated to yield approximately 84.0 mg of green oily liquid designated SB2 (Azwanida, 2015; Sirin, 2025).

The purity of SB2 was assessed by thin-layer chromatography (TLC) in multiple solvent systems, where it consistently showed a single spot (Rf = 0.42 in n-hexane/ethyl ethanoate 9:1, v/v), indicating chromatographic homogeneity under the conditions employed. While TLC is a standard preliminary purity assessment in phytochemical isolation, we acknowledge that advanced techniques such as HPLC would provide more definitive purity confirmation (Ardrey, *et al.;* 2003, D'Atri, *et al*., 2019, Sherma, 2019). The present study therefore reports SB2 as a major isolated fraction exhibiting chromatographic homogeneity under TLC conditions (Urbain *et al*.; 2020).

RESULTS AND DISCUSSION

Characterization and Spectroscopic Data of Compound SB2

Compound SB2 was isolated as a green oily liquid. The ^{1}H NMR spectrum (400 MHz, $CDCl_3$, δ ppm) displayed a complex pattern of signals characteristic of a highly substituted organic molecule with overlapping proton environments (Claridge, 2016).

The spectrum showed two singlets at δ 0.826 and 0.837 (each integrating for 3H), attributable to methyl groups (Silverstein *et. al.,* 2014). A singlet at δ 3.240 (3H) is consistent with a methoxy (OCH_3) group. In addition, a distinct signal observed at δ 3.977 (3H) is assigned to a methyl peroxyl (–O–OCH_3) substituent attached to the phenyl ring. This downfield chemical shift is consistent with the strong electron-withdrawing effect of the peroxide linkage, as well as the deshielding influence of the aromatic system, both of which reduce electron density around the methyl protons and shift the resonance further downfield. (Pretsch *et al*., 2009)

The aliphatic region (δ 1.00–2.003) exhibited multiple overlapping multiplets corresponding to methylene and methine protons within a saturated or partially saturated framework. Due to extensive signal overlap in this region, individual coupling patterns could not be unambiguously resolved (Fulmer *et al*., 2010). The ^{1}H NMR spectrum of SB2 also displays multiple signals in the aromatic region (δ 7.243–7.293), corresponding to approximately six aromatic protons. This observation is inconsistent with a simple disubstituted benzene ring system and instead suggests the presence of a more complex aromatic framework, possibly involving multiple aromatic rings or an extended conjugated system. The close proximity and partial overlap of these signals indicate that the aromatic protons are located in similar chemical environments, making precise assignment of substitution patterns difficult using ^{1}H NMR data alone. (Fulmer *et al*., 2010, Hu *et al.*; 2024)

Overall, the integrated proton signals are consistent with a complex molecular framework, and in reasonable agreement with the molecular formula $C_{36}H_{50}O_3$ obtained from GC–MS analysis (m/z 530.7804). The observed spectral features support the presence of both aliphatic and aromatic domains, along with oxygenated functionalities, consistent with a highly substituted, possibly polycyclic structure (Gottlieb *et al*., 1997). Figure 1 below gives the proton NMR spectrum of SB2.

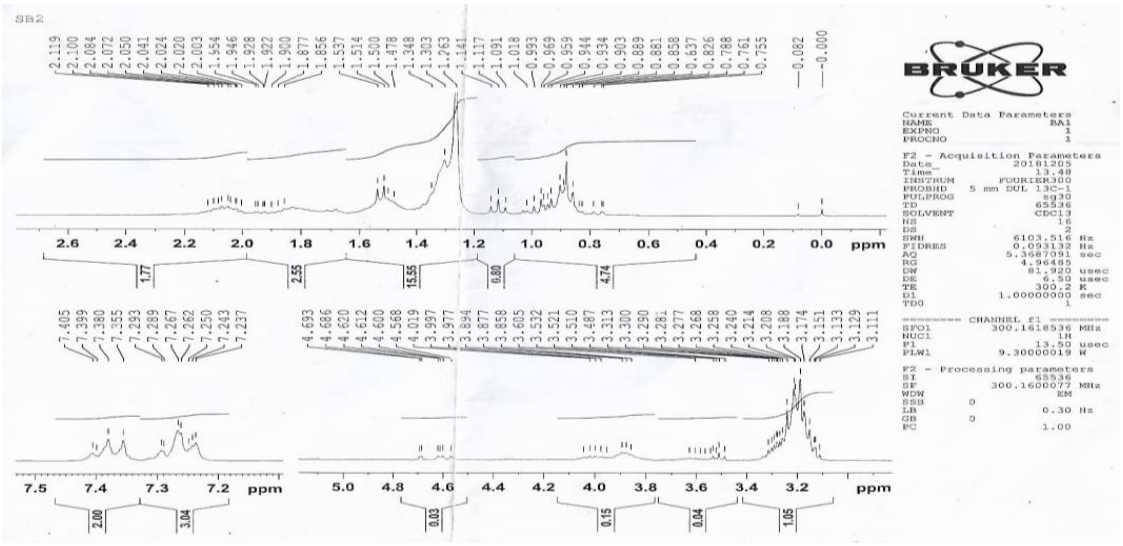

Figure 1: [1]H NMR Spectrum of SB2

The [13]C NMR spectrum (100 MHz, $CDCl_3$, δ ppm) of SB2 exhibited signals predominantly in the aliphatic region (δ 10.8–32.0), consistent with multiple methyl, methylene, and methine carbons within a saturated framework (Gunawan & Nandiyanto, 2021). Several closely spaced signals observed in this region are indicative of carbons in similar chemical environments, leading to partial overlap (Williamson & Masters, 2016).) Signals in the range δ 50.4–61.4 are attributable to oxygenated carbons, including a methoxy (OCH_3) group. The aromatic region displayed resonances between δ 122.03 and 129.92, corresponding to aromatic CH carbons (Pretsch *et al*.; 2009). Additional downfield signals observed around δ ~149 ppm is consistent with deshielded aromatic or oxygenated carbons (Pavia *et al.,* 2015).

Although numerous signals are observed, some resonances are closely spaced and partially overlapping, which may lead to apparent duplication or overestimation of the number of distinct carbons (Martínez-Ramírez *et al*., 2022; Claridge, 2016). The overall carbon distribution is, however, consistent with the molecular formula $C_{36}H_{50}O_3$ obtained from GC–MS analysis (Abdullahi *et al*. 2025). Figure 2 below shows the [13]C NMR spectrum of SB2, while Table 1 presents the corresponding [1]H and [13]C NMR data.

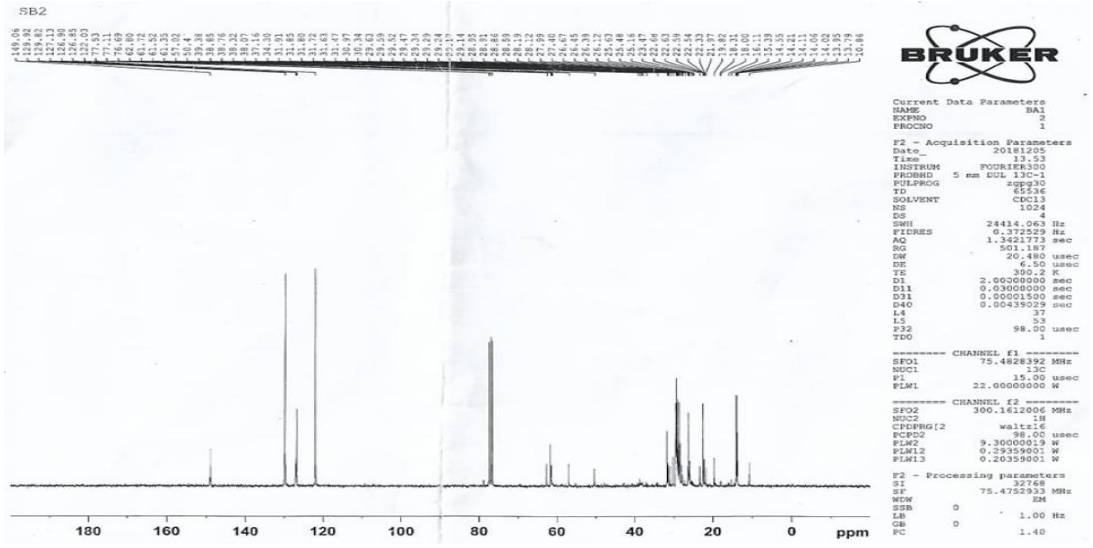

Figure 2: [13]C NMR Spectrum of SB2

Table 1: [1]H and [13]C NMR Data of SB2

Position	Chemical shift (δC)	Carbon	Type	Chemical shift (δH)	Multiplicity	Proton
12	16.11	$-CH_2$	Aliphatic	1.018	2Hm	$-CH_2$
11	18.00	$-CH_2$	,,	1.091	2Hm	$-CH_2$
10	18.31	$-CH_2$	,,	1.117	2Hm	$-CH_2$
9	25.16	-CH	,,	1.856	1Hm	-CH
9a	50.44	$-O-CH_3$	,,	3.240	3Hs	$-O-CH_3$
8a	25.48	-CH	,,	1.877	1Hm	-CH
8	19.82	$-CH_2$	,,	1.141	2Hm	$-CH_2$
7	21.97	$-CH_2$	,,	1.263	2Hm	$-CH_2$

Position	Chemical shift (δC)	Carbon	Type	Chemical shift (δH)	Multiplicity	Proton
6b	25.48	-CH	,,	1.900	1Hm	-CH
12b	25.63	-CH	,,	1.922	1Hm	-CH
12a	50.44	C	Quaternary	-	-	-
12c	10.86	$-CH_3$	Aliphatic	0.826	3Hs	$-CH_3$
13	22.33	$-CH_2$	,,	1.303	2Hm	$-CH_2$
14	22.54	$-CH_2$	,,	1.348	2Ht	$-CH_2$
14a	57.02	C	Quaternary	-	-	-
14c	13.79	$-CH_3$	Aliphatic	0.837	3Hs	$-CH_3$
6a	26.12	-CH	,,	1.928	1Hm	-CH
6	22.59	$-CH_2$	,,	1.478	2Hm	$-CH_2$
5	22.63	$-CH_2$	,,	1.500	2Hm	$-CH_2$
4a	26.39	-CH	,,	1.946	1Hm	-CH
14b	26.45	-CH	,,	1.954	1Hd	-CH
1	22.68	$-CH_2$	,,	1.514	1Hm	$-CH_2$
2	23.47	$-CH_2$	,,	1.537	2Hm	$-CH_2$
3	26.67	-CH	,,	2.020	1Hm	-CH
4	25.16	$-CH_2$	,,	2.003	2Hm	$-CH_2$
1	122.03	=CH	Aromatic	7.243	1Hm	=CH
2	130.15	=C	Aromatic	-	-	-
3	126.83	=CH	Aromatic	7.250	2Hm	=CH
4	126.90	=CH	Aromatic	7.262	1Hm	=CH
4a	131.15	=C	Aromatic	-	-	-
8a	132.05	=C	Aromatic	-	-	-
5	127.13	=CH	Aromatic	7.267	1Hm	=CH
6	149.06	C	,,	-	-	-
6a	61.35	-O-O-CH_3	Methyl peroxyl	3.977	3Hs	-O-O-CH_3
7	129.82	=CH	Aromatic	7.289	1Hm	=CH
8	129.92	=CH	,,	7.293	1Hm	=CH

The 2D ^1H–^1H COSY spectrum of SB2 revealed correlations primarily within the aliphatic region (δ 1.00–2.20), indicating the presence of coupled methylene and methine proton spin systems characteristic of a saturated or partially saturated framework. These correlations suggest contiguous proton networks within the aliphatic portion of the molecule (Claridge, 2016).

Weak correlations were also observed among aromatic protons in the δ 7.20–7.40 region, consistent with coupling within an aromatic system (Claridge, 2016). However, due to signal overlap and spectral complexity, clear delineation of individual coupling pathways was limited. No definitive long-range correlations between methoxy protons (δ ~3.24 ppm) and distant aliphatic proton signals were established from the COSY spectrum. The methoxy group is therefore interpreted as isolated from the main aliphatic spin systems, consistent with its attachment to a non-protonated carbon centre. (Davies *et al*.; 2026). Figure 3 below shows the COSY (2D ^1H–^1H NMR) spectrum of SB2.

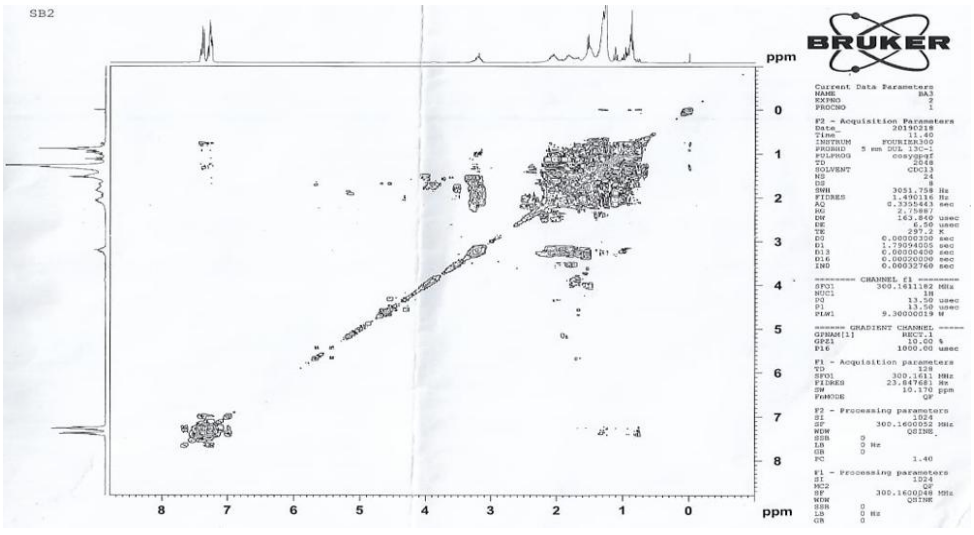

Figure 3: COSY (2D ^1H–^1H NMR) Spectrum of SB2

Functional group identification was achieved using FTIR spectroscopy, while detailed structural elucidation was carried out using NMR and GC–MS techniques. The FTIR spectrum was recorded over the range 4000–400 cm^{-1} (Pavia *et al.,* 2015). The FTIR spectrum of SB2 confirmed the presence of both aromatic and aliphatic structural features together with a peroxide-containing substituent. The absorption band observed at 3067.0 cm^{-1} was assigned to aromatic C=C stretching vibrations, while the bands at 1487.2 and 1481.1 cm^{-1} corresponded to aromatic C–C skeletal vibrations, confirming the presence of benzene rings (Miller *et al.;* 2026). The characteristic aromatic C–H bending vibrations appearing within the range of 675–870 cm^{-1} further supported the aromatic nature of the compound (Silverstein *et al*., 2014). Bands at 2926.0 and 2855.1 cm^{-1} were attributed to aliphatic C–H stretching vibrations, indicating the presence of alkyl groups (Stuart, 2004). The absorption bands within the ranges of 800–950 cm^{-1} and 1000–1150 cm^{-1} were assigned to O–O and C–O stretching vibrations, respectively, characteristic of an aromatic peroxide moiety (CH_3–O–O–) (Nakamoto, 2009). In addition, the band at 1349.3 cm^{-1} corresponded to C–O stretching of an aliphatic ether (methoxy) group, further confirming the presence of a methoxy substituent in the structure of SB2 (Nakamoto, 2009). Figure 4 below gives the FTIR spectrum of SB2 and Table 2 outlines the Infra-red analysis of SB2.

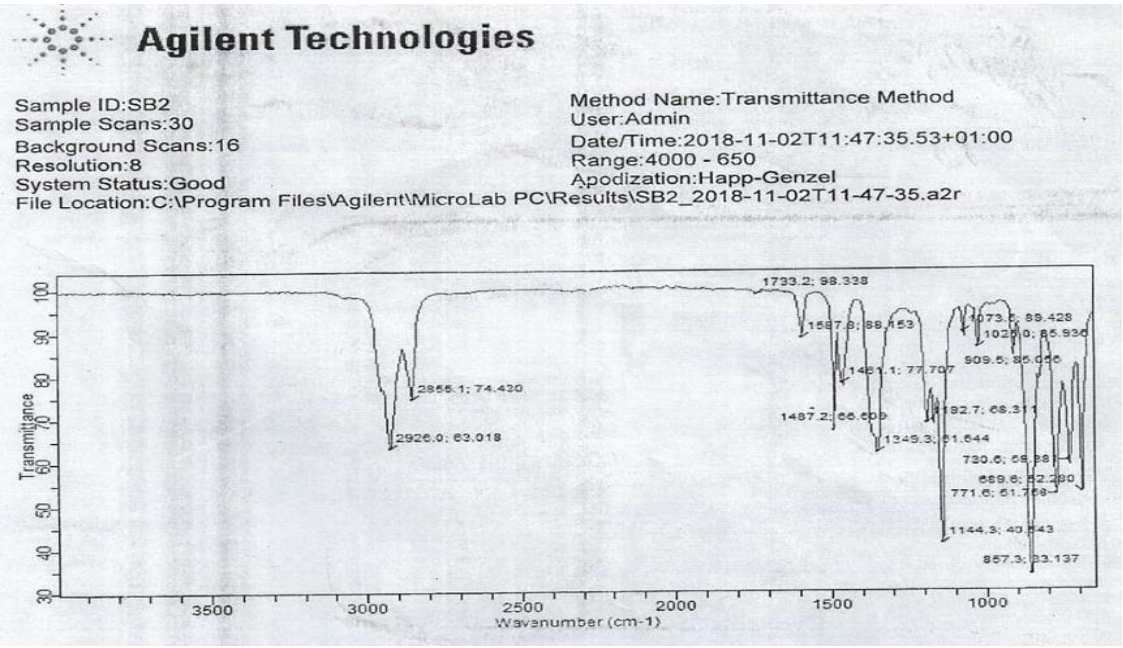

Figure 4: FTIR Spectrum of SB2

Table 2: Infra-red Analysis of SB2

IR absorption (cm^{-1})	Functional group	Compound type
3067.0	C=C	Aromatic
2926.0	C–H	Aliphatic
2855.1	C–H	Aliphatic
800 – 950 (O – O stretch), 1000-11150 (C – O stretch)	CH_3 – O – O -	Aromatic peroxide
1349.3	C-O	Aliphatic ether
1487.2	C-C	Aromatic
1481.1	C-C	Aromatic
675-870	C-H	Aromatic

The GC–MS (EI) spectrum of SB2 displayed a molecular ion peak at m/z 530.7804, consistent with the proposed molecular formula $C_{36}H_{50}O_3$. Prominent fragment ions were observed at m/z 456, 368, 341, and 315, indicating successive fragmentation of the molecular framework. The base peak at m/z 93 suggests the presence of a stable aromatic fragment, supporting the occurrence of an oxygenated aromatic moiety (Chen *et al*., 2023). The fragmentation pattern is in agreement with previously reported spectra of related compounds (Schüler *et al*., 2025; Ma, 2022; Mika'llu *et al*; 2025). Figure 5 below gives the GC–MS spectrum of SB2, while Figure 6 gives the fragmentation pattern of SB2.

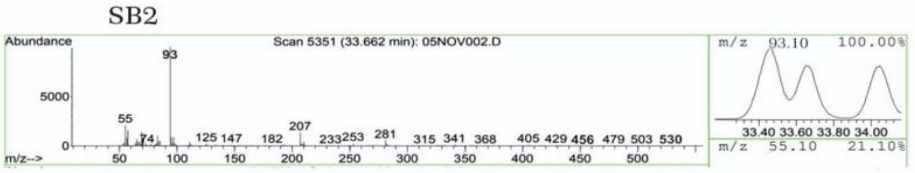

Figure 5: GC–MS Spectrum of SB2

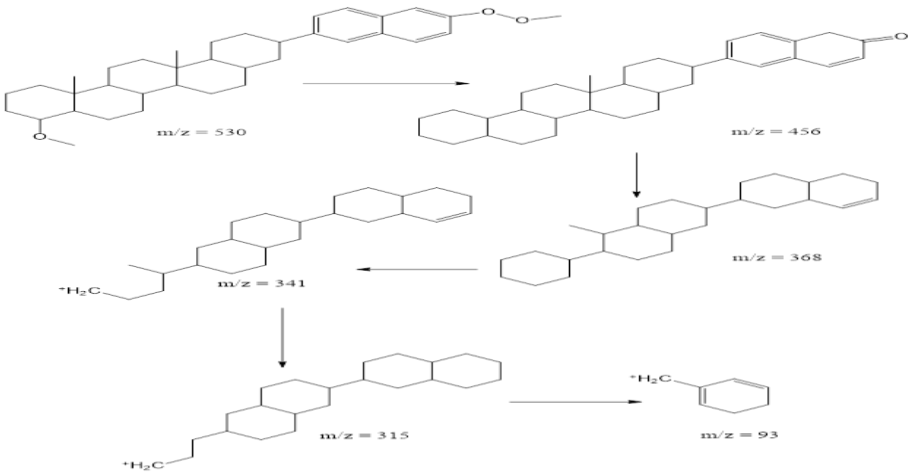

Figure 6: Fragmentation Pattern of SB2

The collective spectroscopic evidence obtained from FTIR, GC–MS, ^{1}H NMR, ^{13}C NMR, and COSY analyses supports the proposed oxygenated aromatic–aliphatic framework of compound SB2. Accordingly, a tentative molecular structure consistent with the observed spectral features and molecular formula ($C_{36}H_{50}O_3$) is shown in Figure 7 below.

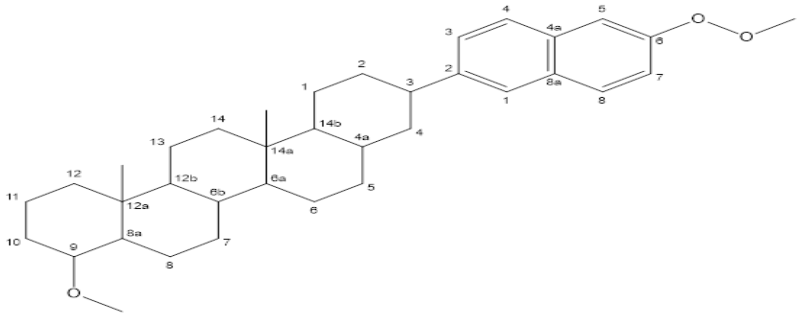

9-methoxy-12a,14a-dimethyl-3-(6-(methylperoxy)naphthalen-2-yl)docosahydropicene

$C_{36}H_{50}O_3$ m/z = 530.7804

Figure 7: Proposed Molecular Structure of SB2

Correlation with Literature and Structural Implications

The spectroscopic features of compound SB2 indicate the presence of both aliphatic and aromatic domains, as well as oxygenated functionalities such as methoxy groups and a methyl peroxyl group as evidenced by FTIR, ^{1}H NMR, and ^{13}C NMR data. The combined presence of these features suggests that SB2 belongs to a class of oxygenated organic compounds incorporating both saturated and conjugated structural elements (Borges *et al.;* 2024).

However, the available spectroscopic data do not allow for definitive classification into a specific structural subclass such as aryl-alkyl ketones or long-chain aromatic ethers (Agatha *et al.;* 2024). Instead, the data are more appropriately interpreted as indicative of a complex molecular framework with multiple chemically similar environments, leading to overlapping signals in both ^{1}H and ^{13}C NMR spectra (Bax and Summers, 1986).

In comparison with previously reported metabolites from *Lactuca* species, such as sesquiterpene lactones (e.g. lactenin and lactucopicrin) and triterpenoids (e.g., taraxasterol), SB2 appears to differ significantly in its molecular mass though there is similarity in spectroscopic profile. While these known compounds typically fall within the C_{15} and C_{30} classes, respectively, the molecular formula $C_{36}H_{50}O_3$ obtained for SB2 suggests a higher level of structural complexity. At present, the biosynthetic origin of such a compound within *Lactuca taraxacifolia* cannot be clearly established and may involve unusual secondary metabolic transformations or mixed biosynthetic pathways (Scott & Piel, 2019).

It is also important to note that certain inconsistencies observed in the spectroscopic data, including overlapping NMR signals and limitations in carbon assignment, restrict the level of structural detail that can be confidently proposed (Breton & Reynolds, 2013; Casanova & Wilson, 2019). Such irregularities may arise from solvent effects, residual impurities, hydrogen-bonding interactions, conformational flexibility, and instrumental resolution limitations, all of which can influence peak appearance, splitting patterns, and signal clarity in NMR spectroscopy (Valentino *et al*.; 2020). In some cases, poor peak separation, broadened resonances, or the presence of residual solvent and moisture peaks may lead to an apparent increase in the number of observed signals despite the compound being structurally consistent with the proposed product (Nazarski, 2023). Furthermore, the structural complexity commonly associated with polycyclic oxygenated compounds may contribute to overlapping resonances, closely spaced chemical shifts, and intricate coupling patterns, thereby complicating definitive spectral interpretation. (Desmet *et al.;* 2021). Although the GC–MS and FTIR data strongly support the presence of the expected functional groups and molecular framework (Sneddon, *et al.;* 2007), the observed NMR limitations necessitate cautious

interpretation of the structural assignments. Additionally, the physical description of the compound as an oily liquid, despite spectral indications of structural complexity, further emphasizes the need for careful evaluation of the analytical data (Pauli, 2014).

Therefore, the combined spectroscopic evidence supports the presence of an oxygenated, possibly polycyclic compound with both aromatic and aliphatic features. Further studies involving advanced spectroscopic techniques such as HSQC and HMBC, which enable direct heteronuclear correlation and long-range connectivity mapping in NMR spectroscopy, would be required for definitive structural elucidation (Bax & Summers, 1986). More recent advances in multidimensional and enhanced-sensitivity NMR methods further support the need for complementary high-resolution techniques in complex molecular systems (Giraudeau, 2023).

CONCLUSION

This study reports the extraction, isolation, and spectroscopic characterization of compound SB2 from the aerial parts of *Lactuca taraxacifolia*. Chromatographic separation of the trichloromethane fraction yielded SB2 as a green oily liquid exhibiting chromatographic homogeneity under TLC conditions. Spectroscopic analyses involving FTIR, ^{1}H NMR, ^{13}C NMR, COSY, and GC–MS revealed that SB2 possesses a structurally complex molecular framework containing both aromatic and aliphatic domains together with oxygenated functionalities, including methoxy and methylperoxy substituents. The molecular ion peak observed at m/z 530.7804 strongly supported the molecular formula $C_{36}H_{50}O_3$, suggesting a highly substituted oxygenated compound with possible polycyclic characteristics.

The FTIR spectrum confirmed the presence of aromatic, aliphatic, peroxide, and ether functionalities, while the NMR spectra indicated multiple overlapping proton and carbon environments consistent with a complex structural arrangement. Although overlapping signals in the NMR spectra limited complete proton and carbon assignments, the GC–MS and FTIR data provided substantial supporting evidence for the proposed oxygenated aromatic–aliphatic framework of SB2. COSY correlations further supported interconnected aliphatic proton systems and aromatic coupling interactions. Collectively, the spectroscopic findings expand the phytochemical knowledge of *Lactuca taraxacifolia* and suggest the presence of a potentially uncommon secondary metabolite within the species.

Nevertheless, the exact structure of SB2 remains tentative and requires further confirmation. Therefore, advanced spectroscopic investigations involving HSQC, HMBC, NOESY, and X-ray crystallography are recommended for definitive structural elucidation. Additional purity confirmation using HPLC analysis is also recommended. Furthermore, biological activity studies including antioxidant, antimicrobial, anti-inflammatory, and cytotoxic evaluations should be conducted to determine the pharmacological relevance of the compound. Comparative phytochemical and metabolomic studies involving related *Lactuca* species may also help clarify the biosynthetic origin and chemotaxonomic significance of SB2 and establish whether it represents a novel natural product or a structurally modified derivative of previously reported metabolites.

REFERENCES

Abdullahi, M. M., Nkemakonam, O. M., Garba, U., & Mustapha, M. A. (2025). Identification and characterization of bioactive compound in *Croton nigritanus* using FTIR and GC–MS spectroscopy. *FUDMA Journal of Sciences*. https://doi.org/10.33003/fjs-2025-09(AHBSI)-1279.

Adinortey M.B., Sarfo J.K., Kwarteng J., Adinortey C.A., Ekloh W., Kuatsienu L.E., Kwadwo Nyarko A. (2018). The Ethnopharmacological and Nutraceutical Relevance of *Launaea taraxacifolia* (Willd.) Amin ex C. Jeffrey. *Evidence-Based Complementary and Alternative Medicine*. 7259146. https://doi.org/10.1155/2018/7259146.

Agatha, O., Mutwil-Anderwald, D., Tan, J. Y., & Mutwil, M. (2024). Plant sesquiterpene lactones. *Philosophical Transactions of the Royal Society B: Biological Sciences*, 379(1914). https://doi.org/10.1098/rstb.2023.0350.

Anyanwu, B. C., Akoh, O. U., & Otuokere, I. E. (2022). Phytochemical screening and proximate analysis of the leaves of *Launaea (Lactuca) taraxacifolia*. *Journal of Chemical Society of Nigeria*, 47(2), 421–432. https://doi.org/10.46602/jcsn.v47i2.737.

Anyanwu, B. C., Otuokere, I. E., Echeme, J. O., Akoh, O. U., Njoku, C. P., Ohenhen, O. N., & Ikeadim, O. C. (2021). Isolation and characterization of a secondary metabolite from the aerial parts *of Launaea (Lactuca) taraxacifolia*. *Journal of Chemical Society of Nigeria*, 46(4), 661–672. https://doi.org/10.46602/jcsn.v46i4.644.

Ardrey, R. E. (2003*). Liquid chromatography–mass spectrometry: An introduction*. John Wiley & Sons. https://doi.org/10.1002/0470867299.

Azwanida, N. N. (2015). A review on the extraction methods uses in medicinal plants, principle, strength and limitation. *Medicinal & Aromatic Plants*, 4(3), 196. https://doi.org/10.4172/2167-0412.1000196.

Bax, A., & Summers, M. F. (1986). ^{1}H and ^{13}C assignments from sensitivity-enhanced detection of heteronuclear multiple-bond connectivity by 2D NMR. *Journal of the American Chemical Society*, 108(8), 2093–2094. https://doi.org/10.1021/ja00268a057.

Borges, R. M., Teixeira, A. M., & Farias, M. A. S. (2024). On the role of NMR in metabolomics and natural product structural analysis. *Frontiers in Natural Products*, 3, 1359151. https://doi.org/10.3389/fntpr.2024.1359151.

Breton, R. C., & Reynolds, W. F. (2013). Using NMR to identify and characterize natural products. *Natural Product Reports*, 30(4), 501–524. https://doi.org/10.1039/c2np20104f.

Chen, L., Pan, H., Zhai, G., Luo, Q., Li, Y., Fang, C., & Shi, F. (2023). Widespread occurrence of in-source fragmentation in the analysis of natural compounds by liquid chromatography–electrospray ionization mass spectrometry. *Rapid Communications in Mass Spectrometry*, 37(12), e9519. https://doi.org/10.1002/rcm.9519.

Claridge, T. D. W. (2016). *High-resolution NMR techniques in organic chemistry* (3rd ed.). Elsevier. https://doi.org/10.1016/C2015-0-04654-8.

D'Atri, V., Fekete, S., Clarke, A., Veuthey, J.-L., & Guillarme, D. (2019). Recent advances in chromatography for

pharmaceutical analysis. *Analytical Chemistry*, 91(1), 210–239. https://doi.org/10.1021/acs.analchem.8b05026.

Davies, E., Morris, G. A., Roy, S. S., & Adams, R. W. (2026). Spin-system-selective 2D *J-spectroscopy*. *Chemistry Methods*, 6(5), e70115. https://doi.org/10.1002/cmtd.70115.

Desmet, S., Morreel, K., & Dauwe, R. (2021). Origin and function of structural diversity in the plant specialized metabolome. *Plants*, 10(11), 2393. https://doi.org/10.3390/plants10112393.

Fulmer, G. R., Miller, A. J. M., Sherden, N. H., Gottlieb, H. E., Nudelman, A., Stoltz, B. M., Bercaw, J. E., & Goldberg, K. I. (2010). NMR chemical shifts of trace impurities: Common laboratory solvents, organics, and gases in deuterated solvents relevant to the NMR spectroscopist. *Organometallics*, 29(9), 2176–2179. https://doi.org/10.1021/om100106e.

Giraudeau, P. (2023). Quantitative NMR spectroscopy of complex mixtures. *Chemical Communications*, 59, 6627–6642. https://doi.org/10.1039/D3CC01455J.

Gottlieb, H. E., Kotlyar, V., & Nudelman, A. (1997). NMR chemical shifts of common laboratory solvents as trace impurities. *The Journal of Organic Chemistry*, 62(21), 7512–7515. https://doi.org/10.1021/jo971176v.

Grootveld, M., Percival, B., Gibson, M., Osman, Y., Edgar, M., Molinari, M., Mather, M. L., Casanova, F., & Wilson, P. B. (2019). Progress in low-field benchtop NMR spectroscopy in chemical and biochemical analysis. *Analytica Chimica Acta*, 1067, 11–30. https://doi.org/10.1016/j.aca.2019.02.026.

Gunawan, R., & Nandiyanto, A. B. D. (2021). How to read and interpret ^{1}H-NMR and ^{13}C-NMR spectrums. *Indonesian Journal of Science and Technology*, 6(2), 267–298. https://doi.org/10.17509/ijost.v6i2.34189.

Harborne, J. B. (1998). *Phytochemical methods: A guide to modern techniques of plant analysis* (3rd ed.). Springer.

Hu, F., Chen, M. S., Rotskoff, G. M., Kanan, M. W., & Markland, T. E. (2024). Accurate and efficient structure elucidation from routine one-dimensional NMR spectra using multitask machine learning. *arXiv*. https://arxiv.org/abs/2408.08284.

Koukoui, O., Agbangnan, P., Boucherie, S., Yovo, M., Nusse, O., Combettes, L., & Sohounhloué, D. (2015). Phytochemical study and evaluation of cytotoxicity, antioxidant and hypolipidemic properties of *Launaea taraxacifolia* leaves extracts on cell lines HepG2 and PLB985. *American Journal of Plant Sciences*, 6(11), 1768–1779. https://doi.org/10.4236/ajps.2015.611177.

Lebeda, A., Doležalová, I., Feráková, V., & Astley, D. (2004). Geographical distribution of wild Lactuca species (Asteraceae, Lactuceae). *The Botanical Review*, 70(3), 328–356. https://doi.org/10.1663/0006-8101(2004)070[0328:gdowls]2.0.Co;2.

Lovestead, T., & Urness, K. (2019). Gas chromatography–mass spectrometry (GC–MS). In ASM handbook (Vol. 10, Materials characterization). *ASM International*. https://tsapps.nist.gov/publication/get_pdf.cfm?pub_id=926655.

Ma, X. (2022). Recent advances in mass spectrometry-based structural elucidation techniques. *Molecules*, 27(19), 6466. https://doi.org/10.3390/molecules27196466.

Martínez-Ramírez, J. A., González, M. A., López, J. P., & Fernández, R. (2022). Novel nuclear magnetic resonance method for position-specific carbon isotope analysis of organic molecules with significant impurities. *Analytical Chemistry*, 94(43), 15124–15131. https://doi.org/10.1021/acs.analchem.2c03356.

Mika'Ilu, H., Sani, A., Suleiman, S., Sani, I., Abdullahi, K. B., Hamisu, A., & Wad, K. H. (2025). Extraction, isolation, characterization and phytochemical screening of Euphorbia balsamifera leaf extract for pesticidal activity against Callosobruchus maculatus. *FUDMA Journal of Sciences*, 9(AHBSI), 160–170. https://doi.org/10.33003/fjs-2025-09(AHBSI)-3411.

Miller, L. M., & Coates, J. P. (2026). Interpretation of infrared spectra: A practical and systematic approach. In R. A. Meyers (Ed.), *Encyclopedia of analytical chemistry* (pp. 10815–10837). Wiley. https://doi.org/10.1002/9780470027318.a5606.pub2.

Nakamoto, K. (2009). *Infrared and Raman spectra of inorganic and coordination compounds: Part A: Theory and applications in inorganic chemistry* (6th ed.). John Wiley & Sons. https://doi.org/10.1002/9780470405840.

Nazarski, R. B. (2023). On the use of deuterated organic solvents without TMS to report ^{1}H/^{13}C NMR spectral data of organic compounds: Current state of the method, its pitfalls and benefits, and related issues. *Molecules*, 28(11), 4369 https://doi.org/10.3390/molecules28114369.

Newman, D. J., & Cragg, G. M. (2020). Natural products as sources of new drugs over the nearly four decades from 01/1981 to 09/2019. *Journal of Natural Products*, 83(3), 770–803. https://doi.org/10.1021/acs.jnatprod.9b01285.

Nikolin, B., Imamović, B., Medanhodzić-Vuk, S., & Sober, M. (2004). High performance liquid chromatography in pharmaceutical analyses. *Bosnian Journal of Basic Medical Sciences*, 4(2), 5–9. https://doi.org/10.17305/bjbms.2004.3405.

Pauli, G. F., Chen, S. N., Simmler, C., Lankin, D. C., Gödecke, T., Jaki, B. U., Friesen, J. B., McAlpine, J. B., & Napolitano, J. G. (2014). Importance of purity evaluation and the potential of quantitative ^{1}H NMR as a purity assay. *Journal of Medicinal Chemistry*, 57(22), 9220–9231. https://doi.org/10.1021/jm500734a.

Pavia, D. L., Lampman, G. M., Kriz, G. S., & Vyvyan, J. R. (2015). *Introduction to spectroscopy* (5th ed.). Cengage Learning.

Pretsch, E., Bühlmann, P., & Badertscher, M. (2009). *Structure determination of organic compounds: Tables of spectral data* (4th ed.). Springer. https://doi.org/10.1007/978-3-540-93810-1.

Salazar-Gómez, A., Ontiveros-Rodríguez, J. C., Pablo-Pérez, S. S., Vargas-Díaz, M. E., & Garduño-Siciliano, L. (2020). The potential role of sesquiterpene lactones isolated from

medicinal plants in the treatment of the metabolic syndrome – A review. *South African Journal of Botany*, 135, 240–251. https://doi.org/10.1016/j.sajb.2020.08.020.

Schüler, J. A., Kramell, A. E., Schmidt, A., Walesch, P. D., & Csuk, R. (2025). Prediction of fragmentation pathway of natural products, antibiotics, and pesticides by ChemFrag. *Journal of Mass Spectrometry*, 60(5), e5129. https://doi.org/10.1002/jms.5129.

Scott, T. A., & Piel, J. (2019). The hidden enzymology of bacterial natural product biosynthesis. *Nature Reviews Chemistry*, 3(7), 404–425. https://doi.org/10.1038/s41570-019-0107-1.

Sherma, J. (2019). Thin-layer chromatography in the determination of synthetic and natural colorants in foods. *In Advances in Chromatography* (pp. 109–135). https://doi.org/10.1201/9780429026171-4.

Silverstein, R. M., Webster, F. X., Kiemle, D. J., & Bryce, D. L. (2014). *Spectrometric identification of organic compounds* (8th ed.). Wiley. https://doi.org/10.1002/9781119134637.

Sirin O. (2025). Preparative chromatography: Fundamentals, applications, and differences from analytical chromatography. Amasya Üniversitesi, Suluova Meslek Yüksekokulu, Gıda İşleme Bölümü. https://orcid.org/0000-0002-4620-7483.

Sneddon, J., Masuram, S., & Richert, J. C. (2007). Gas chromatography–mass spectrometry—Basic principles, instrumentation and selected applications for detection of organic compounds. *Analytical Letters*, 40(6), 1003–1012. https://doi.org/10.1080/00032710701300648.

Stuart, B. H. (2004). Infrared spectroscopy: Fundamentals and applications. John Wiley & Sons. https://doi.org/10.1002/0470011149.

Urbain, A., & Avello Simões-P, C. (2020). *Thin-layer chromatography for the detection and analysis of bioactive natural products*. In Encyclopedia of Analytical Chemistry. John Wiley & Sons. https://doi.org/10.1002/9780470027318.a9907.pub2.

Valentino, G., Graziani, V., D'Abrosca, B., Pacifico, S., Fiorentino, A., & Scognamiglio, M. (2020). NMR-based plant metabolomics in nutraceutical research: An overview. *Molecules*, 25(6), 1444. https://doi.org/10.3390/molecules25061444.

Williamson, K. L., & Masters, K. M. (2016). *Macroscale and microscale organic experiments* (7th ed.). Cengage Learning.